
Property-Guided Generative Modelling for Robust Model-Based Design with Imbalanced Data

Saba Ghaffari¹Ehsan Saleh¹Alexander G. Schwing^{1,2}Yu-Xiong Wang¹Martin D. Burke³ Saurabh Sinha^{1,4}Department of Computer Science, University of Illinois Urbana-Champaign¹Department of Electrical and Computer Engineering, University of Illinois Urbana-Champaign²Department of Chemistry, University of Illinois Urbana-Champaign³Department of Biomedical Engineering, Georgia Institute of Technology⁴{sabag2, ehsans2, aschwing, yxw, mdburke}@illinois.edu
saurabh.sinha@bme.gatech.edu

Abstract

The problem of designing protein sequences with desired properties is challenging, as it requires to explore a high-dimensional protein sequence space with extremely sparse meaningful regions. This has led to the development of model-based optimization (MBO) techniques that aid in the design, by using effective search models guided by the properties over the sequence space. However, the intrinsic imbalanced nature of experimentally derived datasets causes existing MBO approaches to struggle or outright fail. We propose a property-guided variational auto-encoder (PGVAE) whose latent space is explicitly structured by the property values such that samples are prioritized according to these properties. Through extensive benchmarking on real and semi-synthetic protein datasets, we demonstrate that MBO with PGVAE robustly finds sequences with improved properties despite significant dataset imbalances. We further showcase the generality of our approach to continuous design spaces, and its robustness to dataset imbalance in an application to physics-informed neural networks.

1 Introduction

Designing protein sequences with a desired function or property is a challenging problem as the space of protein sequences grows exponentially with the protein length L , which makes exhaustive exploration infeasible in both laboratory and computational settings. Furthermore, most of the protein sequence space is not functional, which exacerbates the difficulty of finding the target sequence. To circumvent this problem, the directed evolution technique [1, 2] has been widely adopted. In this greedy approach, first a set of variants of a naturally occurring ("wild type") sequence are tested for the desired property (assumed to be numerically quantifiable), then the variants with improved property form the starting points of the next round of mutations are selected uniformly at random. This process is repeated until an adequately high level of desired property is achieved. Despite advances, this strategy remains costly and laborious, prompting the development of machine learning techniques that support more efficient exploration of the sequence space [3].

Two directions have been explored for machine learning-assisted directed evolution: (i) using sequence-to-property regression models (oracles) instead of experimental measurements of the property [4–6]; and (ii) performing a more targeted search over the protein sequences guided by the protein properties instead of a random greedy search [7–9]. The methods developed for the latter category use model-based optimization (MBO) for the design problem (model-based design

(MBD)). MBO optimizes the parameters of a search model over the sequence space to maximize an objective assessing the property of interest, e.g., protein fitness [10, 11]. Any search model can be used for MBO, e.g., variational auto-encoders (VAE) [12], and it does not require a differentiable property oracle. Prior work [7, 8] has focused on oracle uncertainty. But for MBD to be successful, it also has to be robust to the imbalanced distribution of samples from the sequence space, which has not been systematically studied. As regions within the sequence space that expose the desired property are extremely rare, real datasets are commonly overpopulated with sequences lacking the desired property. This demands the development of methods that are robust to the extent of existing imbalance in real datasets.

Hence, in this work, we propose a new MBD approach which uses VAE as its search model. However, different from prior work, our latent space is explicitly structured by property values of the sequences. We hence refer to the proposed approach as a “*Property-Guided Variational Auto-Encoder*” (PGVAE). The imposed structure on the latent space allows our new MBD approach to prioritize the samples with the desired property and consistently find samples with improved properties. It also eliminates the need to weight samples, as is done in prior work. Therefore, in our approach all samples fully contribute to the optimization of the model parameters, which makes it robust to the challenges that arise with weighting in imbalanced data settings.

Through extensive benchmarking on real and semi-synthetic protein datasets we demonstrate the robustness of MBD with PGVAE to the extent of existing imbalance between desirable and undesirable protein sequences, and its superiority over prior methods in guiding the search towards optimal regions of the space. Our approach is general and not limited to protein sequences, i.e., discrete design spaces. We further investigate MBD with PGVAE on continuous designs spaces. In an application to physics-informed neural networks (PINN) [13], we showcase that our method can consistently find improved high quality solutions given PINN-derived solution sets overpopulated with low quality solutions to different degrees. Finally, a univariate bimodal Gaussian mixture oracle is used to illustrate the robustness of our MBD with PGVAE to 1) an imbalance ratio of samples taken from the two modes of the oracle distribution, 2) the distance between training samples and the global optimum, and 3) the distance between the two modes, i.e., difference of means, of the oracle.

2 Preliminaries: Model Based Optimization

Given (x, y) pairs as the data points, e.g., protein sequence x and its associated property y (e.g., pKa value), the goal of MBO is to find proteins $x \in \mathcal{X}$ that satisfy an objective S regarding its property with high probability. This objective can be defined as maximizing the property value y , i.e., $S = \{y | y > y_m\}$ where y_m is some threshold. Representing the search model with $p_\theta(x)$ (with parameters θ), and the property oracle as $p_\beta(y|x)$ (with parameters β), MBO is commonly performed via an iterative process which consists of the following three steps at iteration t [11]:

1. Taking K samples from the search model, $\forall i \in \{1, \dots, K\} \quad x_i^t \sim p_{\theta^t}(x)$;
2. Computing sample-specific weights using a monotonic function f which is method-specific:

$$w_i := f(p_\beta(y_i^t \in S | x_i^t)); \quad (1)$$

3. Updating the search model parameters via weighted maximum likelihood estimation:

$$\theta^{t+1} = \arg \max_{\theta} \sum_{i=1}^K w_i \log(p_\theta(x_i^t)). \quad (2)$$

The last step optimizes for a search model that assigns higher probability to the data points satisfying the property objective S , i.e., where $p_\beta(y \in S | x)$ is high. Previous studies [8, 7] have discussed variants of function f to compute the weights to address issues associated with oracle uncertainty.

It is noteworthy that uneven weights can substantially decrease the effective sample size for training, which results in poorly trained model parameters. In imbalanced datasets, such sample weights (w_i) are typically uneven. As an example, assume a dataset of size 100 with five positive (desired property values), and 95 negative (undesired) samples. One weighting scheme can assign non-zero weights to the five desired samples and zero weights otherwise. Therefore, only five out of 100 samples contribute to the objective in Equation 2. This leads to higher bias and variance in the maximum likelihood estimator θ^{t+1} (MLE). Next, we present the same argument mathematically.

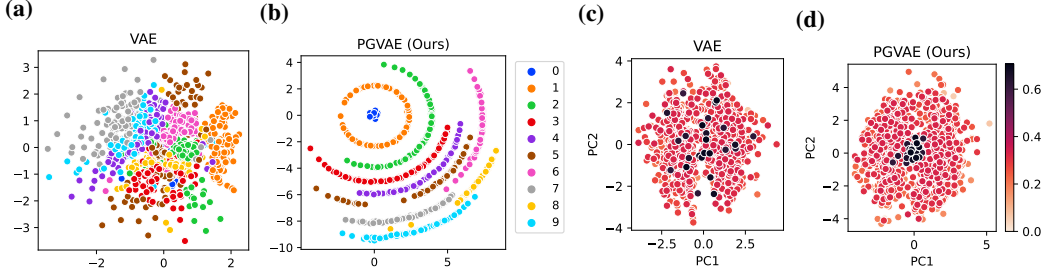


Figure 1: **Latent space structure of PGVAE (ours) vs. vanilla VAE.** **(a) and (b):** VAE and PGVAE with two-dimensional latent space were trained on the MNIST [18] dataset with synthetic property value $(10 - C)$ for digit class C and rare representation of digit zero (sample size ratio $\rho = 0.01$ relative to the sample size of other digits). The samples are scattered in the VAE latent space regardless of their property, whereas PGVAE maps digits with higher property values to circles closer to the origin. **(c) and (d):** PCA representation for 20-dimensional latent spaces of VAE and PGVAE trained on a protein dataset [19] containing a rare population of sequences with property values > 0.5 . VAE scatters the sequences over the space regardless of their property, where as PGVAE maps sequences with higher properties closer to the origin.

Representing the log-likelihood $\log(p_\theta(x_i))$ of the generative model with l_i , Equation 2 can be rewritten as maximizing

$$l = \sum_{i=1}^K w_i l_i. \quad (3)$$

Assuming $\sum_{i=1}^K w_i = 1$ and i.i.d. samples, the effective sample size N_{eff} [14] can be defined such that

$$\text{Var}(l) = \frac{1}{N_{\text{eff}}} \text{Var}(l_i). \quad (4)$$

According to Equation 3, $N_{\text{eff}} = (\sum_{i=1}^N w_i^2)^{-1}$. It can be proved that $1 \leq N_{\text{eff}} \leq K$ where the equality for the lower and upper bound holds at

$$\begin{aligned} N_{\text{eff}} &= K, \quad \forall i, w_i = \frac{1}{K}, \quad \text{and} \\ N_{\text{eff}} &= 1, \quad w_j = 1, \quad w_{i \neq j} = 0. \end{aligned} \quad (5)$$

As mentioned earlier, uneven weights are expected in imbalanced datasets. As the weights become more uneven, N_{eff} approaches its lower bound. Therefore, with imbalanced datasets, N_{eff} tends to drop and $\text{Var}(l)$ increases [15]. This in turn increases the estimation bias ($\mathcal{O}(N_{\text{eff}}^{-1})$) and variance ($\mathcal{O}(N_{\text{eff}}^{-1})$) of the MLE θ^{t+1} [16, 17].

Our search model PGVAE does not require weighting of the samples. Instead, it directly uses the property values to restructure the latent space that gives rise to the samples. Specifically, we encourage samples with better properties to have a higher chance of being generated. For this reason PGVAE has $N_{\text{eff}} = K$ reducing the issues regarding high bias and variance in parameter estimation.

3 Property-Guided Variational Auto-Encoder

PGVAE is a VAE [12] with a special structure imposed on its latent space. The latent space is structured such that samples with the desired property have higher probability of being generated under the vanilla VAE sampling distribution $\mathcal{N}(0, I)$. Representing the encoder and its parameters with Q and θ , the structural constraint on N samples is imposed by

$$\forall (\mu_\theta^i, \mu_\theta^j), \quad i, j \in \{1, \dots, N\} \quad \log(\Pr(\mu_\theta^i)) - \log(\Pr(\mu_\theta^j)) = \tau(y_i - y_j), \quad (6)$$

where $\mu_\theta^i = Q_\theta(x_i)$ and y_i are the latent space representation and property value of sample x_i , respectively. The probability of the encoded representation is $\Pr(\mu_\theta^i) \propto \exp(\frac{-\mu_\theta^{iT} \mu_\theta^i}{2})$ which is compared to the vanilla VAE prior distribution $P(z) := \mathcal{N}(0, I)$ over the latent space. Intuitively, if

higher values of property y are desired, then $y_j \leq y_i$ results in sample i getting mapped closer to the origin. This results in a higher probability of generating sample i than sample j . The extent of prioritization between each pair of samples is controlled by the hyper-parameter τ , often referred to as the temperature. The structural constraint is incorporated into the objective of a vanilla VAE as a relationship loss that should be minimized. This loss is defined as,

$$\mathcal{L}_r \propto \sum_{i,j} \|\log(\Pr(\mu_\theta^i)) - \log(\Pr(\mu_\theta^j)) - \tau(y_i - y_j)\|_2^2. \quad (7)$$

Combined with the vanilla VAE, the final objective of PGVAE to be maximized is,

$$\mathbb{E}_{z \sim Q(\cdot|x)} [\log(P(x|z)) - D_{\text{KL}}(Q(z|x)\|P(z))] - \frac{\lambda_r}{\tau^2} \mathcal{L}_r, \quad (8)$$

where λ_r is a hyper-parameter controlling the extent to which the relationship constraint is enforced. Here, we abused the notation and wrote $Q(z|x)$ for $\Pr(z|Q(x))$. To understand the impact of the structural constraint on the mapping of samples in the latent space, we define $q_i := \log(\Pr(\mu_\theta^i)) - \tau y_i$. Also, assume that the samples are independent and identically distributed (i.i.d.). Then minimizing the relationship loss can be rewritten as

$$\mathcal{L}_r \propto \mathbb{E}_{q_i, q_j} ((q_i - q_j)^2) = \mathbb{E}_{q_i, q_j} (((q_i - \mathbb{E}(q_i)) - (q_j - \mathbb{E}(q_j)))^2). \quad (9)$$

Note that this is related to the variance. Concretely,

$$\mathcal{L}_r \propto 2\text{Var}(q_i) = 2\text{Var}(\log(P(\mu_\theta^i)) - \tau y_i) = 2\text{Var}(-\frac{\mu_\theta^{i^T} \mu_\theta^i}{2} - \tau y_i). \quad (10)$$

Therefore minimizing \mathcal{L}_r is equivalent to,

$$\forall i, \quad \frac{\mu_\theta^{i^T} \mu_\theta^i}{2} = C - \tau y_i, \quad (11)$$

where C is a constant. Equation 11 implies the distribution of samples with the same property value to be on the same sphere which lies closer to the origin for the samples with higher property values. This ensures that higher property samples have higher probability of generation under the VAE prior $N(0, I)$ while allowing for all samples to fully contribute to the optimization, i.e., $N_{\text{eff}} = K$.

An example of the two-dimensional latent space of a PGVAE is shown for the MNIST [18] dataset in Figure 1b. Here we use synthetic property values ($y_i^c = N(10 - c, 10^{-2})$, $\forall c \in \{0, \dots, 9\}$). Digits with smaller scores lie on circles farther from the origin which reduces their probability of generation, whereas digit zero, with sample size ratio $\rho = 0.01$ (imbalance ratio) relative to other digits, is mapped closest to the origin with highest probability of generation. Importantly, this result differs significantly from the latent space of a vanilla VAE, which is illustrated in Figure 1a: the zero digit latent representations lie farther from the origin (also see Figure A2) and are scattered among other digits. Another example of a 20-dimensional latent space for a protein dataset [19] demonstrates that PGVAE maps sequences with higher property values (> 0.5) closer to the origin, as expected. This is illustrated in Figure 1d and Figure A1. Compared to the latent space of a vanilla VAE for the same dataset, shown in Figure 1c, PGVAE concentrates the points with higher property closer to the origin.

4 Experiments

We evaluated the performance of MBD with PGVAE in finding samples with improved properties on eight datasets consisting of 1) three real and three semi-synthetic protein datasets, 2) PINN-derived solutions to the Poisson equation, and 3) a univariate bi-modal Gaussian mixture oracle. Our method is benchmarked against CbAS [8], the state-of-the-art MBO approach robust to oracle uncertainty, and RWR (Reward Weighted Regression) [20] which was used in the benchmarking of CbAS [8]. As the first iteration in MBO is always performed with uniform weights for all samples, we also included as an additional baseline first-weighted RWR (fw-RWR) which performs weighted optimization in the first step as well.

The performance of all methods is evaluated by the maximum property achieved over the union of samples generated in MBO. Additionally, we provide the 75-percentile and 95-percentile of the

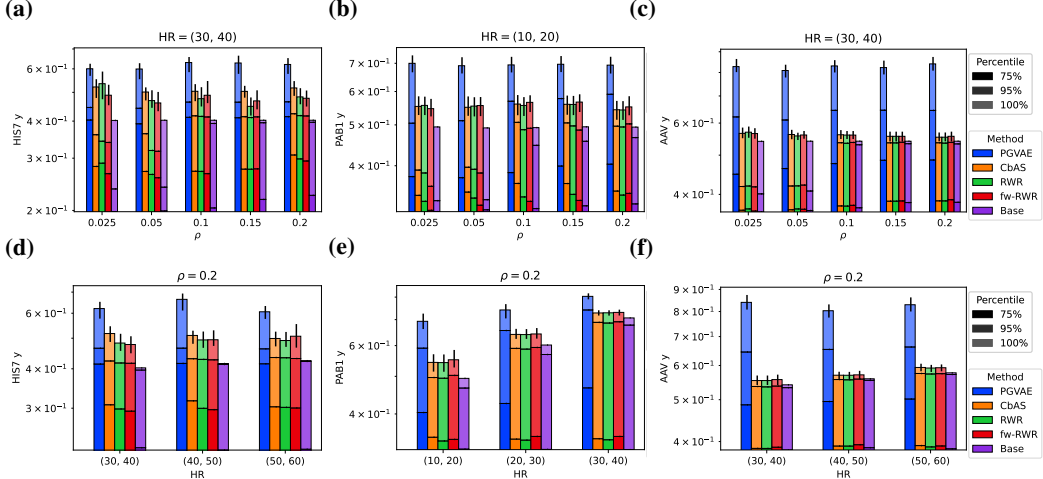


Figure 2: **Model-based design with PGVAE is robust to dataset imbalance on real protein datasets.** (a)(b)(c) For each protein, train sets were generated by taking samples from a fixed low range (LR) ($0, X_l$ -percentile) and high range (HR) (X_{h_1} -percentile, X_{h_2} -percentile) of property values such that $X_l < X_{h_1}$ (**HR** := (X_{h_1}, X_{h_2})) is written in the title. See Appendix for **LR**). Our PGVAE robustly finds the highest property sequence (y-axis) among all methods, regardless of the imbalance ratio ρ between the sample sizes of LR and HR. (d)(e)(f) For a fixed $\rho = 0.2$, PGVAE finds the highest property sequence regardless of the variable HR, which captures the difference between the maximum property existing in the train set and the global optimum of the property which is one. The property percentiles of the training set are represented as the **Base** method.

property values over the same sets. These statistics are averaged over 10 or 50 runs of each method with different random seeds (see Appendix). We also report the 95% confidence interval for the maximum property value.

In all experiments, the training datasets contains a mix of two sets of sampled points (from the entire dataset) with different mean properties. We measure the performance of models under varying imbalance and varying difference in mean properties between the two sets. Furthermore, as the focus of this work is to study robustness of MBD to dataset imbalance, in all experiments we assume the presence of an unbiased oracle. The VAE architecture was dataset-specific (with variable latent space dimension $\in \{2, 10, 20\}$) and the same for all methods (see Appendix). The learning rate was set to 0.001 and the temperature hyper-parameter τ of PGVAE was set to five for all experiments.

4.1 PGVAE performs a robust model-based design on imbalanced protein datasets

Real protein datasets. We perform MBO on three real protein datasets, named here as HIS7 [21], PAB1 [19], and AAV [22]. These datasets have also been utilized in prior computational work in the protein domain [23, 6]. Each dataset consists of protein sequences, i.e., variants of a wild-type sequence, and their measured property, e.g., protein fitness, that has to be optimized over the sequence space. Without loss of generality, we use the generic term "property" for all datasets (see Appendix). The property values in each dataset were transformed to fall within the range (0, 1). As for the property oracle, a ground-truth oracle was used which assigns real property values for the generated sequences that exist in the dataset and zero otherwise. This implies that the search space of the generative model is constrained and a successful MBD method should find the optimum ($y_{\max} = 1$) within a sequence subspace.

Training sets were constructed by taking samples with properties falling in two non-overlapping ranges of property values, which we refer to as low and high ranges. The low range (LR := $(0, X_l$ -percentile)) of property is fixed, while the high range (HR := $(X_{h_1}$ -percentile, X_{h_2} -percentile)) can vary (see Appendix for details). The greater the distance between LR and HR, the closer the maximum property in the training set gets to the optimum.

For a fixed HR, we compare the performance of different methods as the imbalance ratio (ρ) between the number of samples from HR and LR varies. In all datasets, PGVAE consistently finds sequences

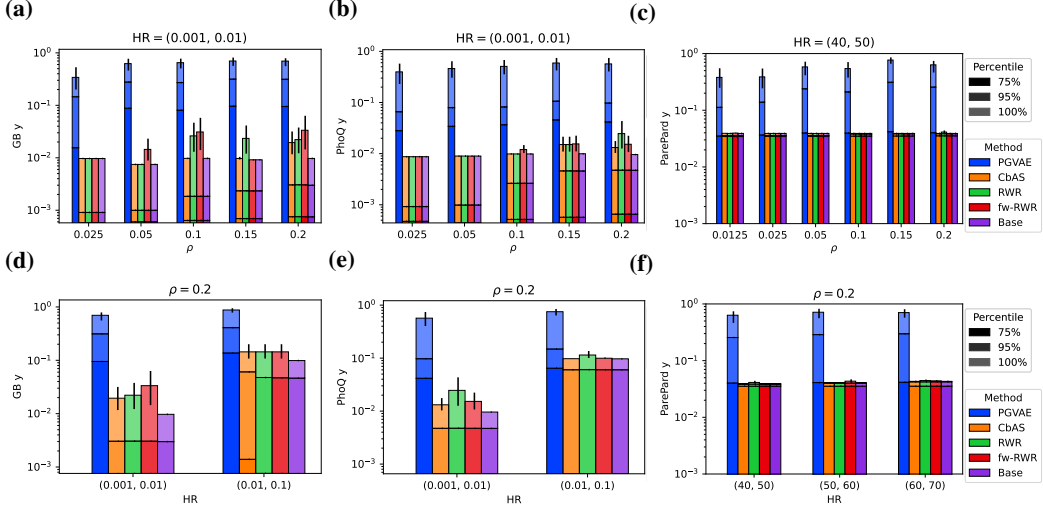


Figure 3: Model-based design with PGVAE is robust to dataset imbalance on semi-synthetic protein datasets. Semi-synthetic datasets were built on real protein datasets to reflect challenging design problems that could exist in practice. (a)(b)(c) For each semi-synthetic protein dataset, train sets were generated by taking samples from a fixed low range (LR) ($0, X_l$) and high range (HR) (X_{h_1}, X_{h_2}) of property values such that $X_l < X_{h_1}$. X_* is either a property value (GB, PhoQ) or a percentile of it (ParePard). PGVAE robustly finds the highest property sequence, regardless of the imbalance ratio ρ between the sample sizes of HR to LR. (d)(e)(f) For a fixed $\rho = 0.2$, PGVAE finds the highest property sequence, regardless of the variable HR which captures the difference between the maximum property existing in the train set and the global optimum of the property which is one.

with higher maximum property values than other methods, regardless of the imbalance ratio (Figures 2a 2b 2c). For a given imbalance ratio ($\rho = 0.2$), PGVAE is robust to varying HR ranges and consistently outperforms other methods (Figures 2d 2e 2f). Notably, for all pairs of (ρ, HR) , PGVAE has better performance with pronounced improvements for the AAV dataset (see Figures A3 A4 A5). The number of samples generated per MBO iteration (N_s) was set to 200 for these experiments. However, the same observations hold with smaller number of samples ($N_s = 100$) in all datasets (see Figures A3 A4 A5).

Semi-synthetic protein datasets. We transformed three real protein datasets to devise challenging yet realistic design problems that exist for protein sequences. We repeated the same benchmark as above on these three semi-synthetic protein datasets that were built upon real protein datasets, named here as GB [24, 25], PhoQ [26, 25] and ParePard [26, 23] (see Appendix). In these datasets we work with a fixed subset of four sites within the protein sequence, with differences among proteins being limited to these sites and with properties transformed to fall within the range $(0, 1)$. We split each dataset into two sets by a threshold on property values which was set to 0.001 in GB and PhoQ, and 30-percentile of property values in the ParePard dataset. The sequences with higher property values (“H set”) were concatenated with a specific 6-length sequence and the sequences with lower properties (“L set”) were concatenated with random 6-length sequences, mimicking the realistic scenario where active proteins have a sequence signature unknown to the oracle.

In challenging protein design problems, there is sparse representation of H set in the dataset. Therefore, we constructed train sets with varying imbalance ratio ρ between samples from H and L sets. Samples from the H set were taken from variable ranges of property values (variable HR) to study the robustness to the difference between the maximum property in the train set and the global optimum 1. To score the generated samples in MBO, we used the ground-truth oracle defined earlier.

Given a fixed HR, PGVAE consistently finds sequences with highest properties among all methods, regardless of the imbalance ratio (Figures 3a 3b 3c). Similarly, given a fixed $\rho = 0.2$, PGVAE finds the highest property sequence and is robust to varying HR ranges (Figures 3d 3e 3f). Similar observations hold for all pairs of (ρ, HR) (see Figures A6 A7). Other methods provide minor improvements as imbalance ratio increases, i.e., easier settings (Figure 3a 3b).

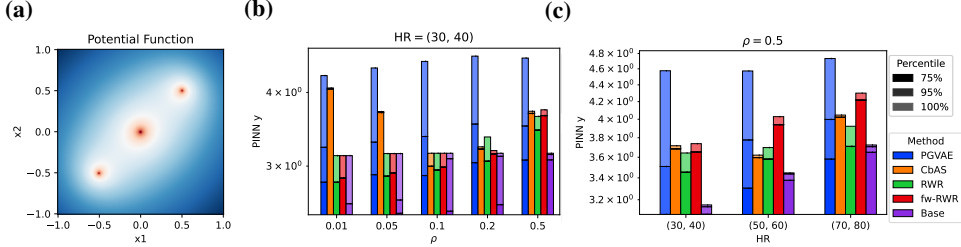


Figure 4: Model-based design with PGVAE robustly finds higher quality solutions given imbalanced PINN-derived solutions to Poisson equation. (a) The analytical solution to the Poisson equation for the potential of three point charges located diagonally in a 2D plane. The goal is to find solutions closer to the analytical solution given an imbalanced dataset of PINN-derived solutions. The property is defined as the negative log MSE between the PINN-derived solution and the analytical solution. (b) train sets were generated by taking samples from a fixed low range (LR) ($0, X_l$ -percentile) and high range (HR) (X_{h1} -percentile, X_{h2} -percentile) of property values such that $X_l < X_{h1}$. Our PGVAE robustly finds higher quality solutions for varying imbalance ratio ρ values. (c) For a given $\rho = 0.5$, PGVAE robustly finds higher quality solutions regardless of HR which can be interpreted as a measure of distance between the highest quality solution in the train set and the target analytical solution. The property percentiles of the training set are represented as the **Base**.

The number of samples generated per MBO iteration (N_s) was set to 200 for these experiments; however, we find the same observations to hold for fewer samples ($N_s = 100$) in all datasets (see Figures A6 A7).

In summary, PGVAE is robust to dataset imbalance for protein design and its advantages are substantial for the more challenging types of protein design problems.

4.2 PGVAE robustly finds higher-quality solutions given imbalanced PINN-derived solution sets to Poisson equation

In previous experiments on proteins, the design space (\mathcal{X}) was discrete. To showcase the generality of our approach, we performed MBD with PGVAE for high-dimensional continuous design spaces. We used a dataset of solutions to the Poisson equation derived from PINNs trained with multiple seeds at different training epochs. Figure 4a shows the analytical solution to the Poisson equation for the potential of three point charges located diagonally on a 2D plane. Negative log weighted MSE between the PINN-derived solution and the analytical solution was used as the property value. Therefore, the goal is to find solutions with higher properties. The analytical solution was used as the oracle which provides exact property values. Similar to the previous benchmarks, solution sets for training were generated by taking samples with properties falling in two ranges (LR and HR) of property value percentiles with different means. The HR variable can be interpreted as how close the best solution in the training set is to the analytical solution.

For a fixed HR, PGVAE robustly finds higher-quality solutions than other methods, regardless of the imbalance ratio, as shown in Figure 4b. For the least $\rho = 0.01$, CbAS is competitive with PGVAE, however its performance is not robust to changes in ρ . For a given imbalance ratio $\rho = 0.5$, PGVAE consistently finds higher-quality solutions than the other methods for varying HR ranges.

MBO was performed with $N_s = 250$ for these experiments. See Figure A8 for performance comparison on all pairs of (ρ, HR) and different N_s values.

4.3 Ablation study of model-based design with PGVAE on Gaussian mixture models

To gain deeper insights into PGVAE’s advantages, we performed a MBD benchmark on an easy-to-understand design space \mathcal{X} , choosing a univariate bimodal Gaussian Mixture Model (GMM) as the property oracle. A univariate bimodal GMM is defined by two sets of parameters (μ_1, σ_1, w_1) and (μ_2, σ_2, w_2) . In all experiments the oracles are designed such that $\mu_1 = 0, \mu_2 > \mu_1$ and $w_2 > w_1$. As $\mu_1 = 0$, the difference between the means ($\Delta\mu = \mu_2 - \mu_1$) of the two modes is controlled by μ_2 .

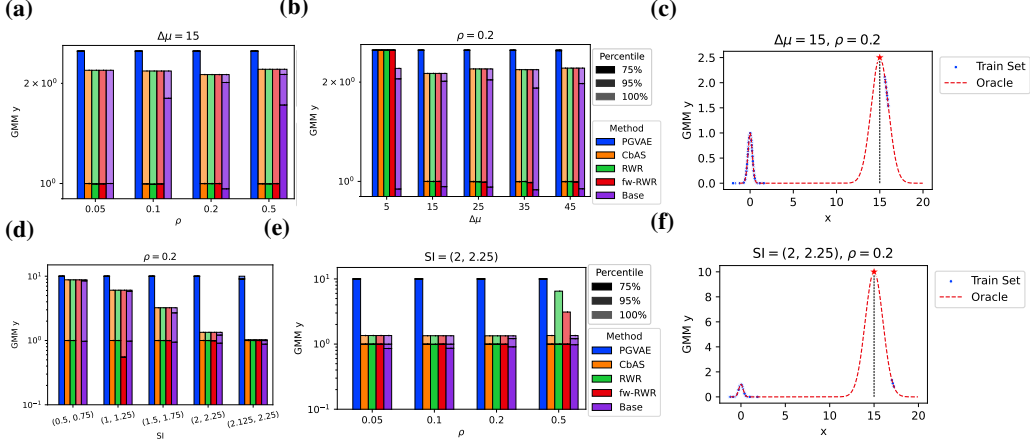


Figure 5: Model-based design with PGVAE is robust to imbalance ratio, distance from global optimum, and the separation of modalities in Gaussian mixture model. Evaluations were done on imbalanced train sets generated from the first (N) and second (ρN) modes of a univariate bimodal GMM. (a) For GMM oracle with $\Delta\mu = 15$, $(w_1, w_2) = (1, 2.5)$, our PGVAE finds the global optimum (2.5) regardless of the imbalance ratio ρ between the samples taken from the two modes. (c) An example of the oracle and train set with $\rho = 0.2$ used in (a). (b) For a fixed imbalance ratio ($\rho = 0.2$), PGVAE robustly finds the global optimum regardless of $\Delta\mu$ which is the extent of separation between the two modes. Other methods can only find optimum when the two modes are closest ($\Delta\mu = 5$). (d) For a given imbalance ratio $\rho = 0.2$ and $\Delta\mu = 15$, PGVAE can robustly find the global optimum (10) regardless of the distance of the sampling interval (SI) from the global optimum. Sampling interval (SI) from the second mode is defined as $(\gamma_s \sigma_2, \gamma_e \sigma_2)$, shifted by μ_2 , with variable pairs of (γ_s, γ_e) . (f) An example of the oracle and a train set with $SI = (2, 2.25)$ used in (d). (e) PGVAE is robust to imbalance ratio and consistently finds global optimum given a fixed $SI = (2, 2.25)$. Only RWR and fw-RWR improves upon the train set for the easiest imbalance ratio setting ($\rho = 0.5$). The property percentiles of the training set are represented as the **Base** method.

Imbalance ratio. To study the impact of the imbalance ratio, train sets were generated by sampling N and ρN points from the first and second modes where $\rho \in \{0.05, 0.1, 0.2, 0.5\}$. The oracle parameters were set to $(\sigma_1, \sigma_2) = (0.25, 1)$ and $(w_1, w_2) = (1, 2.5)$. The sampling distributions were $N(0, 0.6)$ and $\text{Unif}(\mu_2 + \frac{\sigma_2}{2}, \mu_2 + \sigma_2)$ for the first and second modes, respectively. For a given $\mu_2 = 15$, i.e., $\Delta\mu = 15$, PGVAE robustly finds the optimum ($y = 2.5$) regardless of the imbalance ratio, whereas the other methods do not improve upon the maximum in the train set, as shown in Figure 5a. The oracle and a train set example with $\rho = 0.2$ are illustrated for this experiment in Figure 5c.

The same observations hold for other values of $\Delta\mu \geq 15$ as shown in Figure A9. Only for the smallest $\Delta\mu = 5$, baseline methods can also find the global optimum regardless of ρ (see Figure A9) which is expected as the two modes become more proximal.

Separation of modalities $\Delta\mu$. The parameterized GMM allows us to design different oracles by varying $\Delta\mu$. We therefore study the impact of variable $\Delta\mu$ given a fixed imbalance ratio ρ . PGVAE is robust to variations in $\Delta\mu$ and always finds the global optimum of the property, whereas the other methods, as mentioned above, can only find the optimum when the two modes of the oracle are close, i.e., $\Delta\mu = 5$, as shown in Figure 5b.

Distance from the global optimum. Next we examined how distances from the global optimum can affect the performance. GMM parameters $\Delta\mu = 15$, $(\sigma_1, \sigma_2) = (0.25, 1)$, and $(w_1, w_2) = (1, 10)$ were used for these experiments.

The train sets were generated by taking N samples from the first mode and ρN samples from the second mode. To change the distance of the training set from the global optimum (10), the sampling interval (SI) for the second Gaussian was varied to be $SI := (\gamma_s \sigma_2, \gamma_e \sigma_2)$ shifted by μ_2 , where

$$(\gamma_s, \gamma_e) \in \{(0.5, 0.75), (1, 1.25), (1.5, 1.75), (2, 2.25), (2.125, 2.25)\}. \quad (12)$$

Values of (γ_s, γ_e) were chosen so that by increasing γ_s , the samples from the second mode become closer in property value to the samples from the first mode. An example of the oracle and train set is shown in Figure 5f. For a fixed ρ , PGVAE is robust to the sampling interval and always finds the global optimum, whereas other methods fail, as shown in Figure 5d. Similar observations hold for a fixed sampling interval and variable imbalance ratio, as illustrated in Figure 5e. The only exception is RWR and fw-RWR: they improved upon the train set for the highest imbalance ratio which is the easiest setting. See Figure A10 regarding a comparison for all pairs of (SI, ρ) .

The sampling interval is analogous to HR in the aforementioned benchmarks. However, $\Delta\mu$ is a new dimension, which we explored in the GMM experiments and which does not have an analogous counterpart in previous benchmarks. The number of samples generated per MBO iteration (N_s) was set to 200 for these experiments. We find observations also hold for fewer number of samples ($N_s = 100$), as shown in Figures A9 and A10. The oracles and train sets used in the GMM experiments are shown in Figures A11 and A12.

Through a broad array of controlled experiments, we showed the advantage of MBD with PGVAE in imbalanced data regimes. The success of PGVAE is due to its use of property values to restructure the data points within the latent space. Its explicit goal: data points with better property are prioritized over others while maintaining the maximum effective sample size for parameter optimization.

5 Related Work

Machine learning approaches have been developed to improve the design of DNA, molecules and proteins [8, 7, 3, 9, 27, 4]. Recently variants of MBO techniques have been proposed to facilitate the problem of protein design. Specifically, CbAS [8] proposed a weighting scheme which prevents the search model from exploring regions of the design space for which property oracle predictions are unreliable. CbAS [8] was built on an adaptive sampling approach [7] that leverages uncertainty in the property oracle when computing the weights for MBO. Another MBO approach that has been adapted in Reinforcement Learning (RL) and which CbAS [8] was evaluated against is Reward Weighted Regression (RWR) [20] which uses weights that do not take into account oracle uncertainty. Not requiring a differentiable oracle and reliability on weighted optimization are the commonalities of these methods. However, their robustness on challenging imbalanced datasets that exist in real-world applications has yet to be tested.

6 Discussion

We demonstrated the advantages of MBD with PGVAE via a wide array of experiments on real and semi-synthetic protein datasets as well as by improving PINN-derived solutions and GMM samples. In particular, MBD with PGVAE is robust to 1) the extent of imbalance that exists in real-world datasets used for design; 2) the distance from the global optimum defined by the difference of maximum property in the train set and the global optimum; and 3) the distance between the modalities in the design space, which we studied in the context of GMM oracles.

We attribute the success of MBD with PGVAE, in imbalanced data settings, to imposing a structural constraint on the latent space of VAEs such that samples with improved properties are prioritized over others. Hence, they are more likely to be generated by the search model. Unlike other MBO approaches, PGVAE does not require weighting for sample prioritization which makes its parameter optimization robust to imbalanced settings where effective sample size could drop significantly by weighting. We speculate that the drop in effective sample size contributes to the failure of other methods in our studies. It is also possible that the specific weighting scheme could not sufficiently prioritize desired samples over the undesired ones due to the existing imbalance.

Limitations. The structural constraint imposed on the latent space, if optimized perfectly, enforces the samples to lie on spheres centered around the origin. This is restrictive in some problems. Exploration of other forms of structural constraints that allow for property based prioritization of samples is left to future work. Furthermore, we assumed the existence of an unbiased oracle and only studied the issues caused by imbalance for the search model. Our approach can be improved by incorporating strategies that make the search model robust to oracle uncertainties. Finally, in addition to VAEs, other generative models such as GANs and diffusion models can be modified to perform robust MBD in imbalanced data settings, which is an interesting direction for future work.

References

- [1] Keqin Chen and Frances H Arnold. Enzyme engineering for nonaqueous solvents: random mutagenesis to enhance activity of subtilisin e in polar organic media. *Bio/Technology*, 9(11):1073–1077, 1991.
- [2] Andrew Currin, Neil Swainston, Philip J Day, and Douglas B Kell. Synthetic biology for the directed evolution of protein biocatalysts: navigating sequence space intelligently. *Chemical Society Reviews*, 44(5):1172–1239, 2015.
- [3] Rafael Gómez-Bombarelli, Jennifer N Wei, David Duvenaud, José Miguel Hernández-Lobato, Benjamín Sánchez-Lengeling, Dennis Sheberla, Jorge Aguilera-Iparraguirre, Timothy D Hirzel, Ryan P Adams, and Alán Aspuru-Guzik. Automatic chemical design using a data-driven continuous representation of molecules. *ACS central science*, 4(2):268–276, 2018.
- [4] Kevin K Yang, Zachary Wu, and Frances H Arnold. Machine-learning-guided directed evolution for protein engineering. *Nature methods*, 16(8):687–694, 2019.
- [5] Philip A Romero, Andreas Krause, and Frances H Arnold. Navigating the protein fitness landscape with gaussian processes. *Proceedings of the National Academy of Sciences*, 110(3):E193–E201, 2013.
- [6] Yunan Luo, Lam Vo, Hantian Ding, Yufeng Su, Yang Liu, Wesley Wei Qian, Huimin Zhao, and Jian Peng. Evolutionary context-integrated deep sequence modeling for protein engineering. In *Research in Computational Molecular Biology: 24th Annual International Conference, RECOMB 2020, Padua, Italy, May 10–13, 2020, Proceedings 24*, pages 261–263. Springer, 2020.
- [7] David H Brookes and Jennifer Listgarten. Design by adaptive sampling. *arXiv preprint arXiv:1810.03714*, 2018.
- [8] David Brookes, Hahnbeom Park, and Jennifer Listgarten. Conditioning by adaptive sampling for robust design. In Kamalika Chaudhuri and Ruslan Salakhutdinov, editors, *Proceedings of the 36th International Conference on Machine Learning*, volume 97 of *Proceedings of Machine Learning Research*, pages 773–782. PMLR, 09–15 Jun 2019.
- [9] Anvita Gupta and James Zou. Feedback gan for dna optimizes protein functions. *Nature Machine Intelligence*, 1(2):105–111, 2019.
- [10] Mark Zlochin, Mauro Birattari, Nicolas Meuleau, and Marco Dorigo. Model-based search for combinatorial optimization: A critical survey. *Annals of Operations Research*, 131:373–395, 2004.
- [11] Clara Fannjiang and Jennifer Listgarten. Autofocused oracles for model-based design. *Advances in Neural Information Processing Systems*, 33:12945–12956, 2020.
- [12] Diederik P Kingma and Max Welling. Auto-encoding variational bayes. In *Proceedings of the International Conference on Learning Representations*, 2014.
- [13] Maziar Raissi, Paris Perdikaris, and George E Karniadakis. Physics-informed neural networks: A deep learning framework for solving forward and inverse problems involving nonlinear partial differential equations. *Journal of Computational Physics*, 378:686–707, 2019.
- [14] Leslie Kish and Martin Richard Frankel. Inference from complex samples. *Journal of the Royal Statistical Society: Series B (Methodological)*, 36(1):1–22, 1974.
- [15] Art B. Owen. *Monte Carlo theory, methods and examples*. 2013.
- [16] David Firth. Bias reduction of maximum likelihood estimates. *Biometrika*, 80(1):27–38, 1993.
- [17] Saba Ghaffari, Ehsan Saleh, David Forsyth, and Yu-Xiong Wang. On the importance of firth bias reduction in few-shot classification. *International Conference on Learning Representations*, 2022.

- [18] Li Deng. The mnist database of handwritten digit images for machine learning research. *IEEE Signal Processing Magazine*, 29(6):141–142, 2012.
- [19] Daniel Melamed, David L Young, Caitlin E Gamble, Christina R Miller, and Stanley Fields. Deep mutational scanning of an rrm domain of the *saccharomyces cerevisiae* poly (a)-binding protein. *Rna*, 19(11):1537–1551, 2013.
- [20] Jan Peters and Stefan Schaal. Reinforcement learning by reward-weighted regression for operational space control. In *Proceedings of the 24th international conference on Machine learning*, pages 745–750, 2007.
- [21] Victoria O Pokusaeva, Dinara R Usmanova, Ekaterina V Putintseva, Lorena Espinar, Karen S Sarkisyan, Alexander S Mishin, Natalya S Bogatyreva, Dmitry N Ivankov, Arseniy V Akopyan, Sergey Ya Avvakumov, et al. Experimental assay of a fitness landscape on a macroevolutionary scale. *bioRxiv*, page 222778, 2017.
- [22] Drew H Bryant, Ali Bashir, Sam Sinai, Nina K Jain, Pierce J Ogden, Patrick F Riley, George M Church, Lucy J Colwell, and Eric D Kelsic. Deep diversification of an aav capsid protein by machine learning. *Nature Biotechnology*, 39(6):691–696, 2021.
- [23] Adam J Riesselman, John B Ingraham, and Debora S Marks. Deep generative models of genetic variation capture the effects of mutations. *Nature methods*, 15(10):816–822, 2018.
- [24] Nicholas C Wu, Lei Dai, C Anders Olson, James O Lloyd-Smith, and Ren Sun. Adaptation in protein fitness landscapes is facilitated by indirect paths. *Elife*, 5:e16965, 2016.
- [25] Yuchi Qiu and Guo-Wei Wei. Clade 2.0: Evolution-driven cluster learning-assisted directed evolution. *Journal of Chemical Information and Modeling*, 62(19):4629–4641, 2022.
- [26] Anna I Podgornaia and Michael T Laub. Pervasive degeneracy and epistasis in a protein-protein interface. *Science*, 347(6222):673–677, 2015.
- [27] Nathan Killoran, Leo J Lee, Andrew Delong, David Duvenaud, and Brendan J Frey. Generating and designing dna with deep generative models. *arXiv preprint arXiv:1712.06148*, 2017.
- [28] Christopher D Aakre, Julien Herrou, Tuyen N Phung, Barrett S Perchuk, Sean Crosson, and Michael T Laub. Evolving new protein-protein interaction specificity through promiscuous intermediates. *Cell*, 163(3):594–606, 2015.

A Appendix

Table A1 (protein and PINN-derived datasets) and Table A2 (GMM-derived dataset) summarize the different variables used in data generation and studied in the benchmark.

An additional ablation study on the coverage of the undesired GMM oracle mode is shown in Figure A13 and Figure A14. We demonstrate that MBD with PGVAE is robust to the relative coverage of the undesired (first mode) to the desired region (second mode) defined by $\frac{\sigma_1}{\sigma_2}$ where $\sigma_2 = 1$ and σ_1 can vary.

Dataset	Property	Low Range (LR)	High Range (HR)	Imbalance Ratio
HIS7 [21, 23]	selection	(0, 10)%	(30,40), (40,50), (50,60)%	0.025, 0.05, 0.1, 0.15, 0.2
PAB1 [19, 23]	growth	(0, 5)%	(10,20), (20,30), (30,40)%	0.025, 0.05, 0.1, 0.15, 0.2
AAV*[22]	capsid viability	(0, 50*)%	(30, 40), (40, 50), (50, 60)%	0.025, 0.05, 0.1, 0.15, 0.2
GB [24, 25]	fitness	(0.0001,0.001)	(0.001, 0.01), (0.01, 0.1)	0.025, 0.05, 0.1, 0.15, 0.2
PhoQ [26, 25]	fitness	(0.0001,0.001)	(0.001, 0.01), (0.01, 0.1)	0.025, 0.05, 0.1, 0.15, 0.2
ParePard [28, 23]	fitness	(0, 30)%	(40,50), (50,60), (60,70)%	0.0125, 0.025, 0.05, 0.1, 0.15, 0.2
PINN	– log(wMSE)	(0, 15)%	(30, 40), (50, 60), (70, 80)%	0.01, 0.05, 0.1, 0.2, 0.5

Table A1: **Details of the protein and PINN-derived datasets used in the benchmark.** The property name is shown in the Property column. The low range ($0, X_l$) and the high range (X_{h_1}, X_{h_2}) are shown in percentile of the property value for all datasets except GB and PhoQ. In all datasets $X_l \leq X_{h_1}$ except for the AAV dataset. In the AAV dataset, low and high ranges are associated with the nonviable and viable capsid protein sequences.

Dataset	σ_1	σ_2	$\Delta\mu$	Imbalance Ratio (ρ)	Sampling Interval (SI)
GMM	1	1	5, 15, 25, 35, 45	0.05, 0.1, 0.2, 0.5	(0.5, 1)
GMM-SI	1	1	15	0.05, 0.1, 0.2, 0.5	(0.5, 0.75), (1, 1.25), (1.5, 1.75), (2, 2.25), (2.125, 2.25)
GMM-Var	2.5, 5, 10	1	60	0.05, 0.1, 0.2, 0.5	(1.5, 1.75)

Table A2: **Details of the GMM-derived datasets used in the ablation study.** The standard deviations associated with the two modes of GMM oracle are shown in σ_1 and σ_2 columns. The GMM dataset stands for the experiments studying the impact of variable $\Delta\mu$ between the two modes in addition to the imbalance ratio (Figure A9). GMM-SI stands for the experiments studying the impact of variable sampling interval (Figure A10), and GMM-Var shows the experiments that study the impact of variable σ_1 , i.e., extent of the coverage of the undesirable oracle mode, as well as the imbalance ratio (Figure A13).

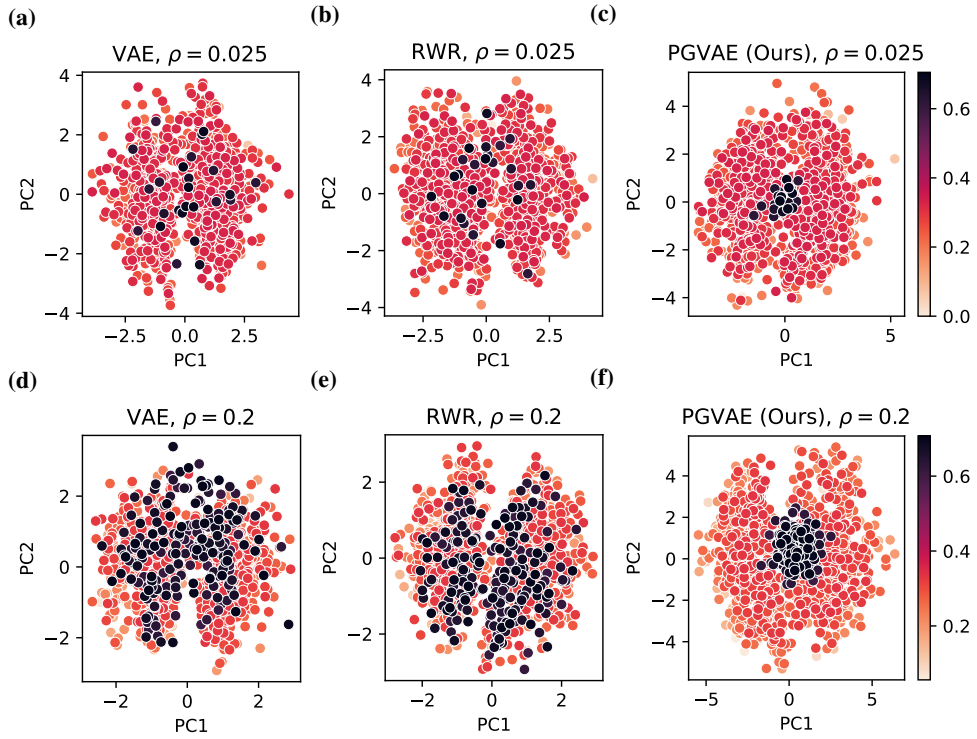


Figure A1: **PCA representation of PGVAE (ours), vanilla VAE and RWR 20-dimensional latent space for PAB1 dataset [19].** Models were trained on two imbalanced datasets with imbalance ratios of 0.2 (a)(b)(c) and 0.025 (d)(e)(f), between sequences with property > 0.5 and the rest. For both imbalance ratios, other methods scatter the samples all around the latent space, whereas PGVAE maps the sequences with higher property closer to the origin. (a) and (c) are the same as (c) and (d) in Figure 1.

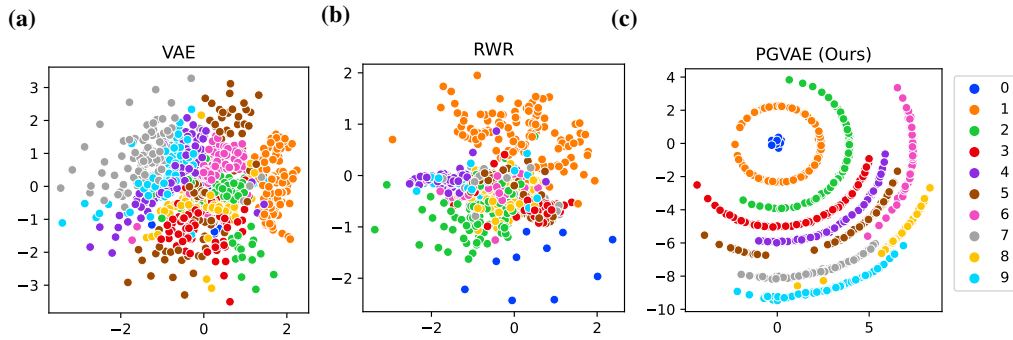


Figure A2: **Two-dimensional latent space for vanilla VAE, RWR, and PGVAE trained on the MNIST [18] dataset with rare representation of digit zero.** (a) and (c) are the same as Figure 1a and Figure 1b. (b) RWR maps samples of zero digit farther from the origin with less probability of generation relative to the other digits, whereas our PGVAE maps zero digit samples closer to the origin than other digits.

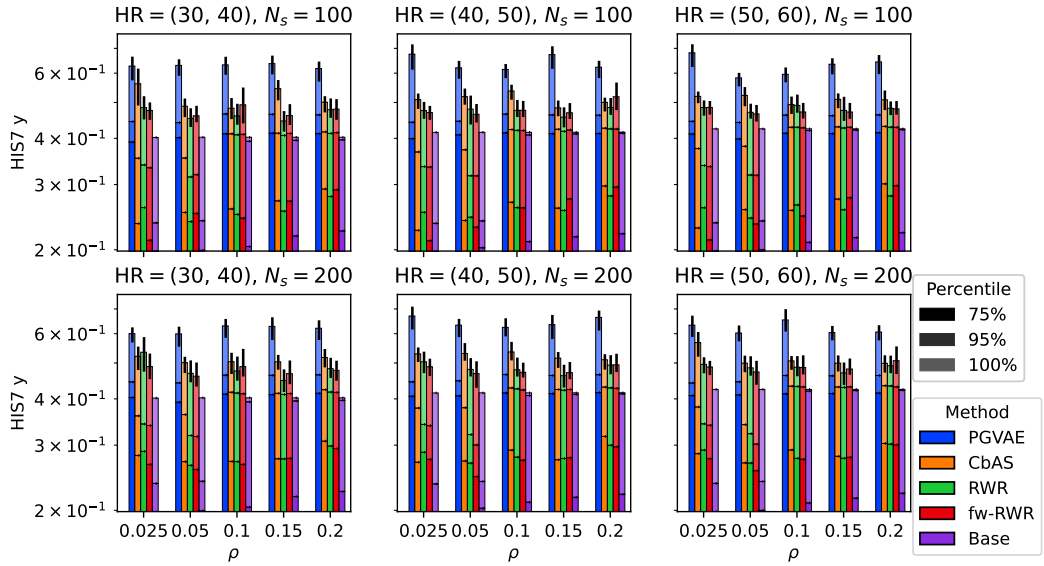


Figure A3: **Model-based design with PGVAE on HIS7 dataset is robust to all combinations of imbalance ratio (ρ), high range (HR), and number of samples (N_s) generated per MBO step.**

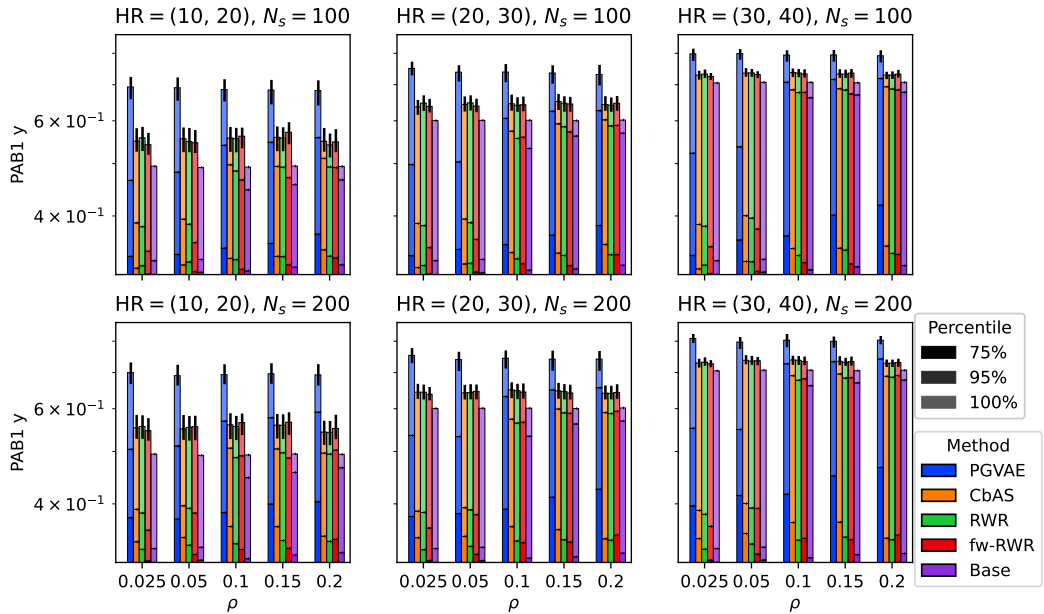


Figure A4: **Model-based design with PGVAE on PAB1 dataset is robust to all combinations of imbalance ratio (ρ), high range (HR), and number of samples (N_s) generated per MBO step.**

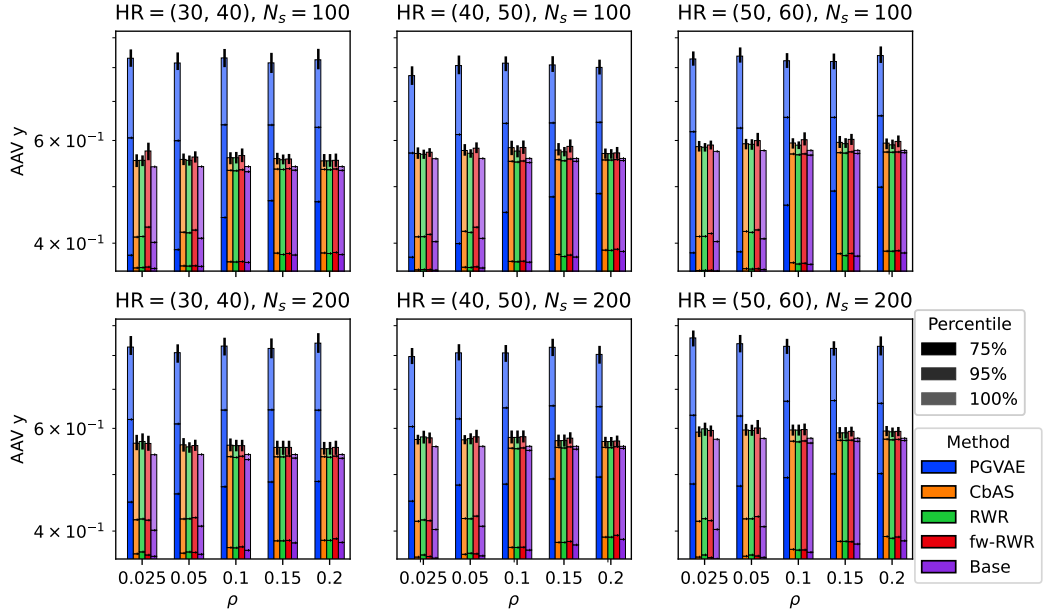


Figure A5: Model-based design with PGVAE on AAV dataset is robust to all combinations of imbalance ratio (ρ), high range (HR), and number of samples (N_s) generated per MBO step.

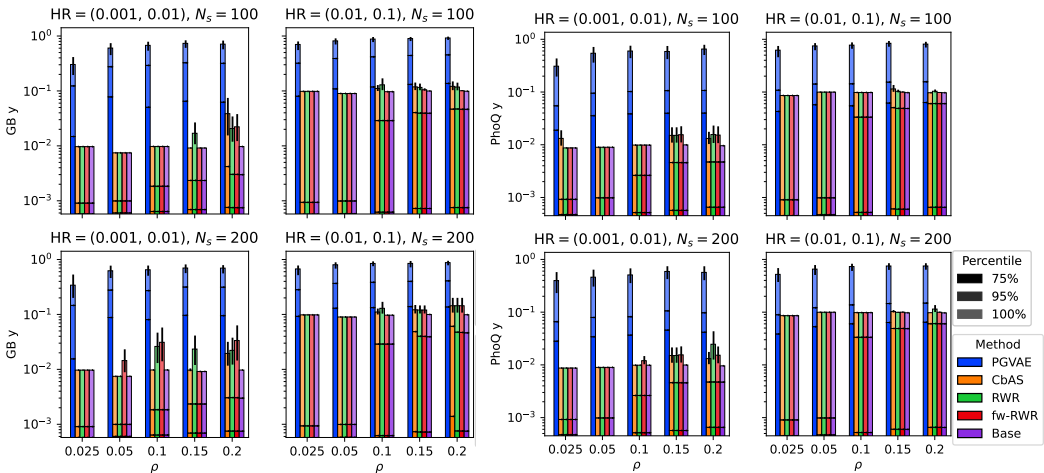


Figure A6: Model-based design with PGVAE on GB (left) and PhoQ (right) datasets is robust to all combinations of imbalance ratio (ρ), high range (HR), and number of samples (N_s) generated per MBO step.

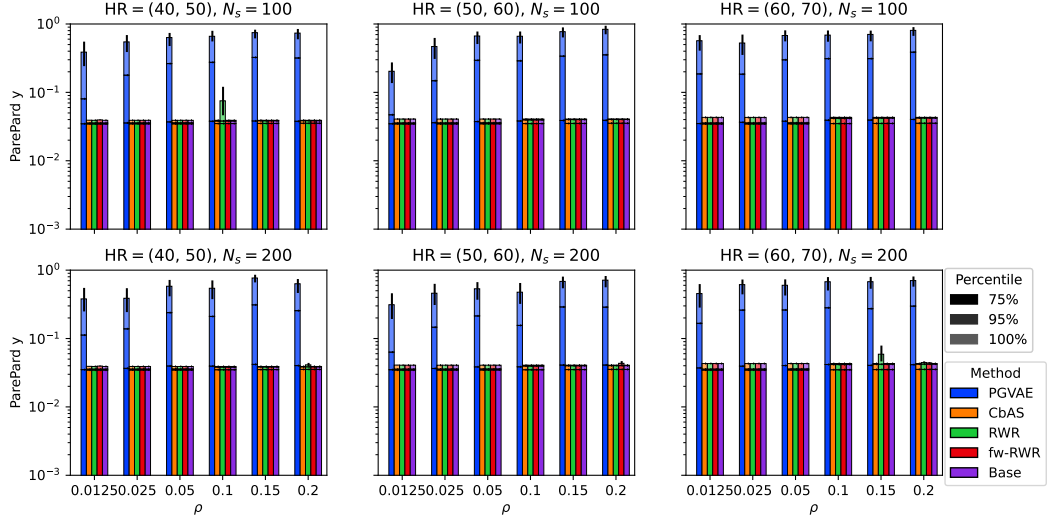


Figure A7: **Model-based design with PGVAE on ParePard dataset is robust to all combinations of imbalance ratio (ρ), high range (HR), and number of samples (N_s) generated per MBO step.**

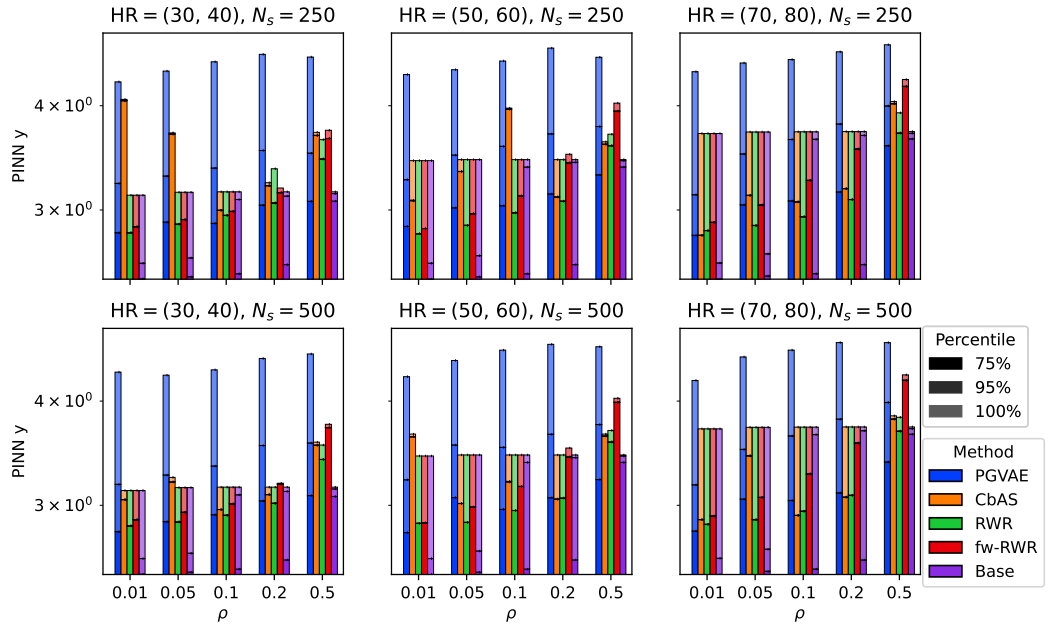


Figure A8: **Model-based design with PGVAE on the imbalanced PINN-derived solution sets is robust to all combinations of imbalance ratio (ρ), high range (HR), and number of samples (N_s) generated per MBO step.**

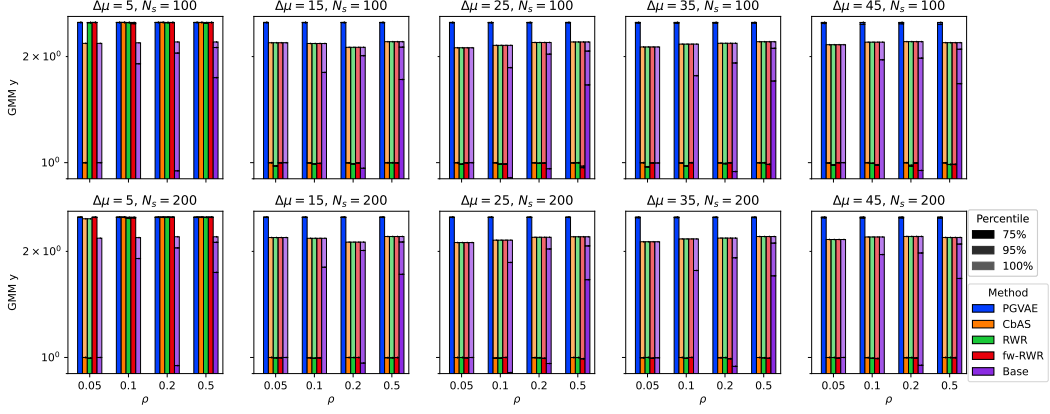


Figure A9: **Model-based design with PGVAE on GMM-derived datasets is robust to all combinations of the imbalance ratio (ρ), difference of the oracle modalities ($\Delta\mu$), and the number of samples generated per MBO step (N_s).**

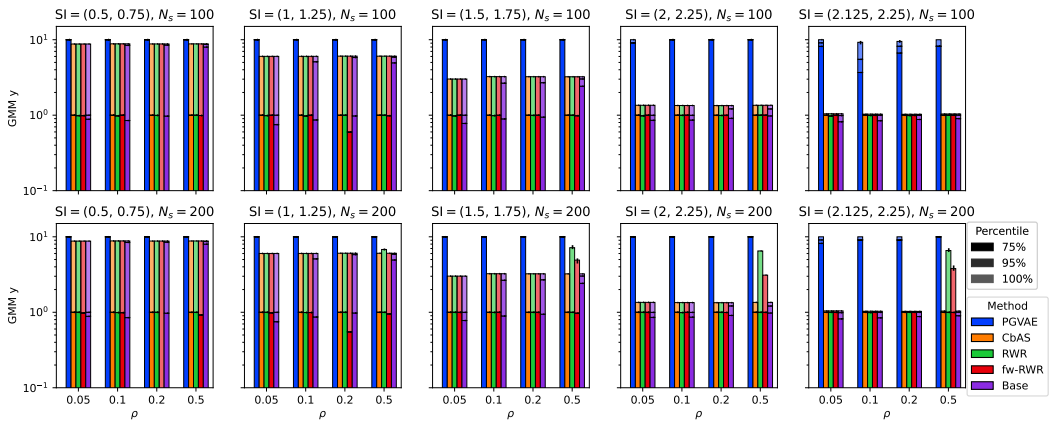


Figure A10: **Model-based design with PGVAE on GMM-derived datasets is robust to all combinations of the imbalance ratio (ρ), sampling interval (SI), i.e., the distance from the global optimum, and the number of samples generated per MBO step (N_s).**

Dataset	VAE Architecture
Protein	indim \rightarrow 64 \rightarrow LReLU \rightarrow 40 \rightarrow 64 \rightarrow LReLU \rightarrow indim
PINN	indim \rightarrow 64 \rightarrow LReLU \rightarrow 20 \rightarrow 64 \rightarrow LReLU \rightarrow indim
GMM	indim \rightarrow 64 \rightarrow LReLU \rightarrow 64 \rightarrow LReLU \rightarrow 4 \rightarrow 64 \rightarrow LReLU \rightarrow 64 \rightarrow LReLU \rightarrow indim

Dataset	Seed Count	MBO N_s
HIS7	10	100, 200
PAB1	50	100, 200
AAV	50	100, 200
GB	10	100, 200
PhoQ	10	100, 200
ParePard	10	100, 200
PINN	10	250,500
GMM	10	100, 200
GMM-SI	10	100,200
GMM-Var	10	100,200

Table A3: **VAE architectures (Left) and MBO settings (Right) used for different datasets. (Left Table)** Protein dataset stands for all real and semi-synthetic protein datasets used in the benchmark. GMM stands for all experiments studying the impact of different variables using the GMM oracle. The latent dimension of the VAE is 20, 10, and 2 for Protein, PINN, and GMM datasets, respectively. **(Right Table)** For each dataset, the number of seeds per MBO run, and the number of samples (N_s) generated per MBO step are represented.

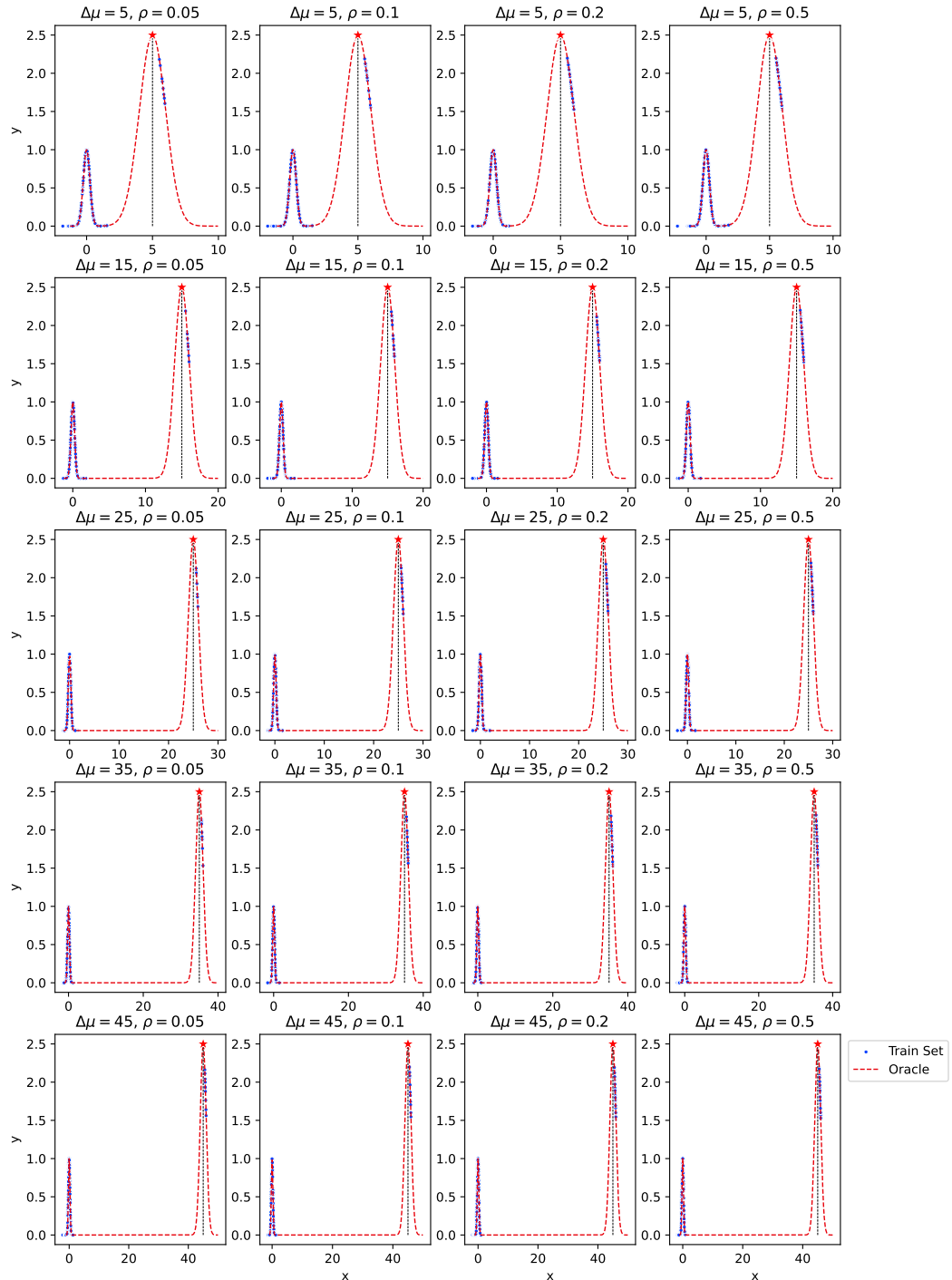


Figure A11: The GMM oracles and training sets associated with GMM dataset in Table A2.

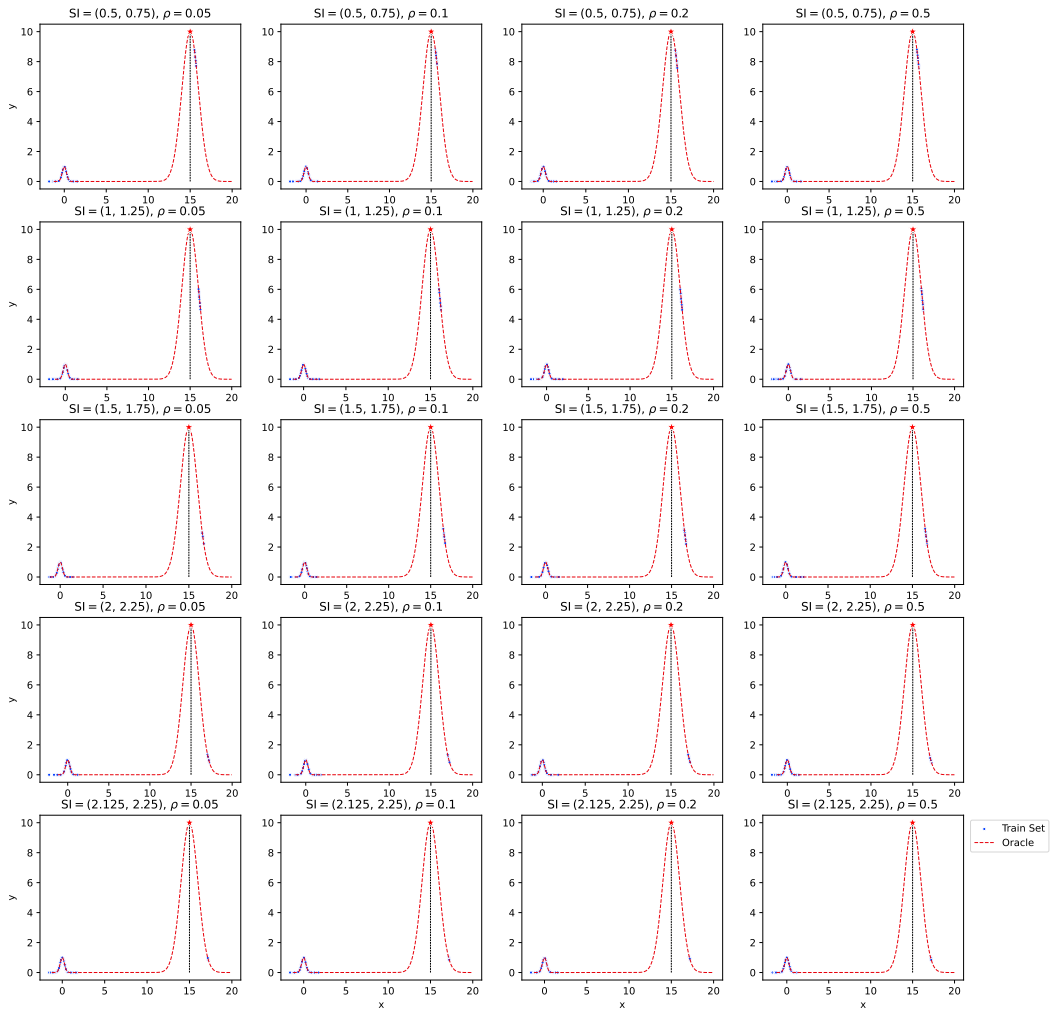


Figure A12: The GMM oracles and training sets associated with GMM-SI dataset in Table A2.

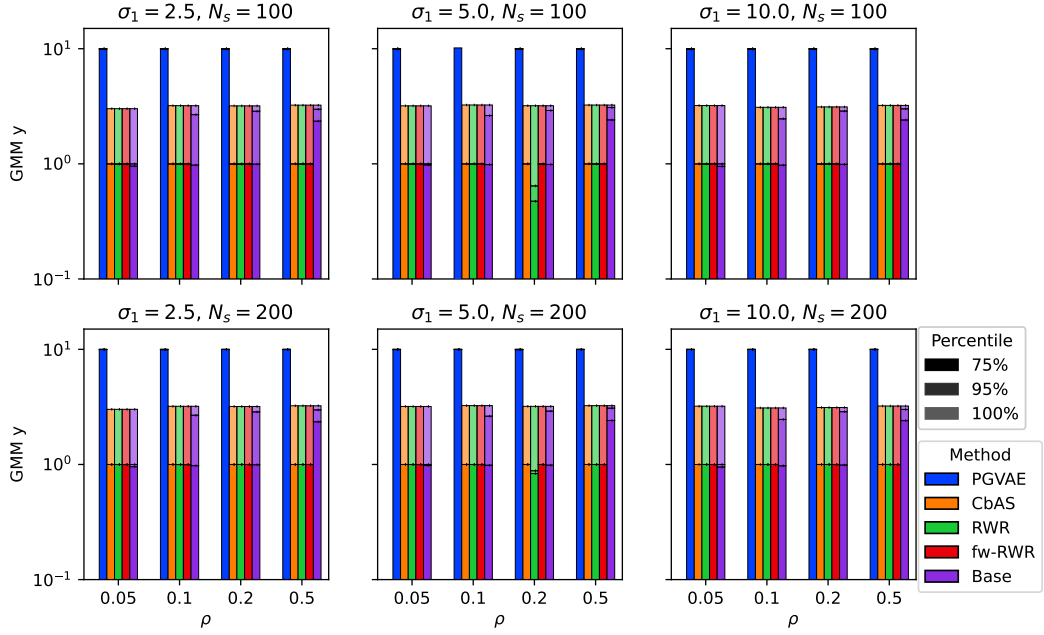


Figure A13: **Model-based design with PGVAE on GMM-derived datasets is robust to all combinations of the imbalance ratio (ρ), extent of the coverage of the undesirable oracle mode defined by σ_1 , and the number of samples generated per MBO step (N_s).**

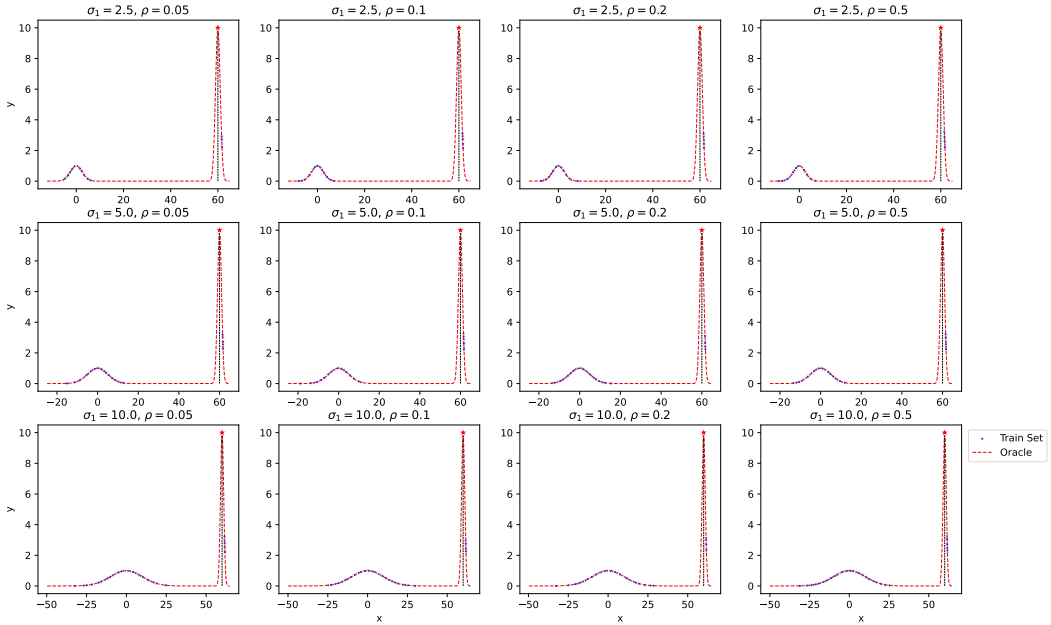


Figure A14: **The GMM oracles and training sets associated with GMM-Var dataset in Table A2.**